

# Versatile method for renormalized stress-energy computation in black-hole spacetimes

Adam Levi and Amos Ori

*Department of physics, Technion-Israel Institute of Technology,  
Haifa 32000, Israel*

We report here on a new method for calculating the renormalized stress-energy tensor (RSET) in black-hole (BH) spacetimes, which should also be applicable to dynamical BHs and to spinning BHs. This new method only requires the spacetime to admit a single symmetry. So far we developed three variants of the method, aimed for stationary, spherically symmetric, or axially symmetric BHs. We used this method to calculate the RSET of a minimally-coupled massless scalar field in Schwarzschild and Reissner-Nordstrom backgrounds, for several quantum states. We present here the results for the RSET in the Schwarzschild case in the Unruh state (the state describing BH evaporation). The RSET is type I at weak field, and becomes type IV at  $r \lesssim 2.78M$ . Then we use the RSET results to explore violation of the weak and null Energy conditions. We find that both conditions are violated all the way from  $r \simeq 4.9M$  to the horizon. We also find that the averaged weak energy condition is violated by a class of (unstable) circular timelike geodesics. Most remarkably, the circular null geodesic at  $r = 3M$  violates the *averaged null energy condition*.

Semiclassical gravity is a theory that describes the interaction of quantum fields with a classical spacetime metric, and their coupled evolution. One of the central goals of semiclassical gravity is to allow detailed understanding of black-hole (BH) evaporation. Since Hawking's discovery in 1974 that BHs emit quantum radiation [1] and evaporate, many efforts have been made to properly formulate and analyze this dynamical process of semiclassical BH evaporation. This phenomenon is directly related to a number of profound issues like the information puzzle and loss of unitarity.

To properly address semiclassical BH evaporation one should (at least in principle) solve the semiclassical Einstein equation [36]

$$G_{\alpha\beta} = 8\pi \langle T_{\alpha\beta} \rangle_{ren}, \quad (1)$$

where  $G_{\alpha\beta}$  is the Einstein tensor and  $\langle T_{\alpha\beta} \rangle_{ren}$  is the quantum field's renormalized stress-energy tensor (RSET). Both sides depend on the evolving spacetime metric  $g_{\alpha\beta}(x)$ , which is the unknown in this equation. The RSET, which emerges from the field's quantum fluctuations, also depends on the type of matter field as well as on its quantum state. Throughout this paper we shall consider a minimally-coupled massless scalar field (MCMSF)  $\phi(x)$ , satisfying  $\square\phi = 0$ .

One of the hardest aspects in dealing with Eq. (1) is the computation of the RSET. In this paper we shall mostly address this aspect: computation of  $\langle T_{\alpha\beta} \rangle_{ren}$  (and analysis thereof) for a prescribed spacetime metric  $g_{\alpha\beta}(x)$ .

In principle, this computation involves summation (and integration) of the contributions to  $\langle T_{\alpha\beta} \rangle$  from the individual field's modes. The naive mode sum is divergent and requires regularization. This is not surprising, as the naive expectation value diverges already in flat spacetime. In flat spacetime, however, one can use the *normal ordering* procedure. Unfortunately, this simple procedure is not applicable in curved spacetime.

Instead, in curved spacetime one can use the *point-splitting* regularization which was developed by DeWitt [2] and later adapted to RSET calculation by Christensen [3]. This procedure is based on formally splitting the evaluation point  $x$  into points  $x$  and  $x'$ , and subsequently taking the limit  $x' \rightarrow x$  while subtracting a known counter-term.

In its naive form the point splitting procedure is practically inapplicable to BH backgrounds: Since in this case the field's modes can only be computed numerically, the naive, direct evaluation of the limit  $x' \rightarrow x$  becomes impractical. To overcome this problem Candelas, Howard, Anderson and others [4–7] developed a version of point-splitting especially adapted to numerical implementation. In their version, the counter-term subtraction and the limit  $x' \rightarrow x$  are analytically translated into certain manipulations applied to the mode contributions upon summation. This method, however, is heavily based on (fourth-order) WKB expansion of the field's modes. It is therefore inapplicable to dynamical backgrounds (such as evaporating BHs), because the WKB expansion becomes tremendously difficult in the time-dependent case. In addition, these methods are in most cases implemented in the Euclidean sector (to circumvent the turning-point problem) — which usually does not exist for time-dependent geometries. The most general case for which this WKB-based method was applied so far was [7] spherically symmetric static background. [8] Furthermore, an Unruh state does not exist in the Euclidean sector, so one has to compute the RSET in a different state (e.g Boulware) in the Euclidean sector and then compute the (convergent) difference between the two states in the Lorentzian sector [37].

Recently we have introduced a new approach to numerically implement point splitting, which does not rely on the WKB expansion. It can therefore be implemented directly in the Lorentzian sector. This method requires the background to admit some symmetry, and the split is

made in the corresponding Killing direction. Our method comes in several versions, depending on the type of symmetry. We first presented the  $t$ -splitting variant, which requires stationarity [13]. More recently we have introduced the angular-splitting (or  $\theta$ -splitting) variant which requires spherical symmetry [14]. And we have also developed the azimuthal-splitting (or  $\varphi$ -splitting) variant which only requires axial symmetry, the details of which will be presented elsewhere [15].

In our approach, instead of using WKB, we extract the required short-distance information directly from Christensen's counter-term. We expand the latter in the appropriate basis functions (Fourier expansion in  $t - t'$  or  $\varphi - \varphi'$  variables for  $t$ - and  $\varphi$ -splittings respectively, and Legendre expansion in  $\theta - \theta'$  for  $\theta$ -splitting [38]). The result of this expansion is then subtracted from the mode contributions, thereby regularizing their sum.

To introduce and illustrate our approach, in Refs. [13, 14] we employed it to compute  $\langle \phi^2 \rangle_{ren}$  (rather than the RSET). This is an easier quantity to compute, being a scalar rather than a tensor, and also being less divergent. This paper reports the successful calculation of  $\langle T_{\alpha\beta} \rangle_{ren}$  using all three variants:  $t$ -,  $\theta$ -, and  $\varphi$ -splittings.

We have used our method to compute the RSET in Schwarzschild and Reissner-Nordstrom backgrounds. Here we focus on the Schwarzschild case, presenting results for a MCMSF in the Unruh state, using all three variants. Previous computations of the RSET in the Unruh state were restricted to conformal fields (scalar [16] and electromagnetic [17]). Here we compute it for the first time (to our knowledge) for a non-conformal field. The details of the RSET calculation in the various splittings will be given elsewhere [15].

One of the interesting aspects of quantum-field RSETs is the extent to which they satisfy or violate various energy conditions. Classical (minimally coupled [39]) matter fields typically satisfy the *weak energy condition* (WEC) which states that no observer can measure negative energy density, namely  $T_{\alpha\beta}u^\alpha u^\beta \geq 0$  for any timelike four-velocity  $u^\alpha$ . Another important energy condition is the *null energy condition* (NEC), which states that every null vector  $k^\alpha$  satisfies  $T_{\alpha\beta}k^\alpha k^\beta \geq 0$ . WEC is stronger than NEC and implies it. Such energy conditions are crucial ingredients in various singularity and horizon theorems [19]. As it turns out, these two purely local conditions are violated by quantum fields even in flat spacetime [20]. Nevertheless, one can also consider averaged conditions. One such important condition is the *averaged null energy condition* (ANEC) which states that every null geodesic  $x^\alpha(\lambda)$  must satisfy

$$\int T_{\alpha\beta}k^\alpha k^\beta d\lambda \geq 0, \quad (2)$$

where  $\lambda$  is an affine parameter and  $k^\alpha \equiv dx^\alpha/d\lambda$ . As it turns out, the ANEC is satisfied [20] in flat spacetime,

and is sufficient for proving several singularity theorems [19] and to enforce topological censorship [21].

It has already been shown that the RSET of quantum electromagnetic field [22] violates ANEC in the Unruh state, and the same for conformal scalar field [23, 24]. For a broader discussion on ANEC violations see [25, 26]. Here we use our RSET results to examine the various energy conditions for a MCMSF in the Unruh state (for first time as far as we know).

*RSET results in the Unruh state.*— The Schwarzschild metric is

$$ds^2 = -(1 - 2M/r) dt^2 + (1 - 2M/r)^{-1} dr^2 + r^2 d\Omega^2,$$

where  $M$  represents the BH mass and  $d\Omega^2 \equiv d\theta^2 + \sin^2\theta d\varphi^2$ . In the background of eternal BH one may consider several distinct vacuum states. The one which best represents the physics outside a realistic evaporating BH is the Unruh state [27]. We computed the RSET in this quantum state using the three aforementioned splitting directions. The results of these three computations agree very well, with typical deviation of order  $10^{-3}$  between  $\theta$ - $t$  splittings, and of order  $10^{-2}$  between  $\theta$ - $\varphi$  splittings. Figure 1 displays all (non-vanishing) components of the RSET [40], calculated in the three variants, as a function of the tortoise coordinate  $r_* = r + 2M \ln(r/2M - 1)$ .

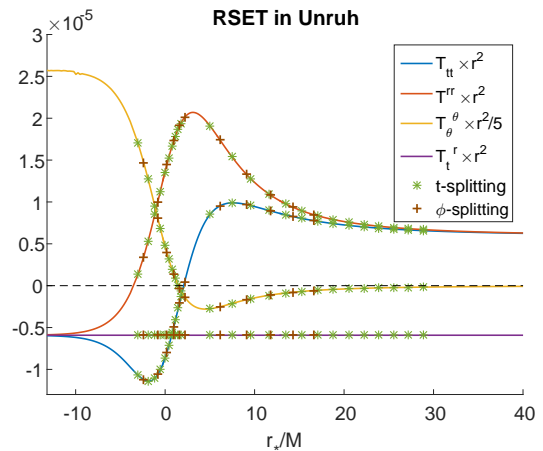


Figure 1: The various components of the RSET in the Unruh state for a MCMSF in Schwarzschild. The curves are the results obtained in  $\theta$ -splitting, the asterisks and plus symbols are results obtained using  $t$ - and  $\varphi$ -splittings respectively. Numerical errors start to increase very close to the horizon (say  $r_* \lesssim -9$ ), which results in the tiny wiggles in  $T_\theta^\theta$ . Note that energy-momentum conservation guarantees that  $r^2 T_t^r = const$ , yielding the straight horizontal solid line.

Since  $\varphi$ -splitting only assumes axial symmetry, in our spherically-symmetric background the RSET may in principle be computed at any desired  $\theta$  value. The results should of course be independent of  $\theta$ , which provides a strong additional consistency check. Here we present

results for  $\theta = \pi/2$ . We point out, however, that in  $\varphi$ -splitting the numerical error typically increases with decreasing  $\theta$ , and it becomes harder to use at, say,  $\theta \lesssim 40^\circ$  (which we hope to improve).

Our resultant RSET satisfies energy-momentum conservation,  $T_{;\beta}^{\alpha\beta} = 0$ . We applied two independent tests to verify this: First, we directly calculated  $T_{;\beta}^{\alpha\beta}$  by applying numerical differentiation to our numerically-computed RSET. Second, we analytically verified that all subtraction terms involved in our mode-sum method do satisfy this conservation law. This is a sufficient check, because the individual mode contributions trivially satisfy energy-momentum conservation.

One of the conservation equations imposes  $r^2 \langle T_t^r \rangle_{ren} = const$ , yielding the straight solid horizontal line in Fig. 1. Integrating this quantity over the two-sphere gives the total energy radiated to infinity  $L = -4\pi r^2 \langle T_t^r \rangle_{ren}$ . Our computation yields  $L = 7.439 \cdot 10^{-5} \hbar M^{-2}$ , which fully agrees with Elster's result [16].

*WEC and NEC analysis.*— The various local energy conditions may conveniently be analyzed through the eigenvalues  $p_\mu$  and eigenvectors  $V_{(\mu)}^\alpha$  ( $\mu = 0, 1, 2, 3$ ) defined by  $T_{\beta}^{\alpha} V_{(\mu)}^\beta = p_\mu V_{(\mu)}^\alpha$ . In spherical symmetry there are always two spacelike eigenvectors  $V_{(2,3)}^\alpha$  in the angular directions, with (real)  $p_2 = p_3$ . The eigenvalue analysis then reduces to the  $2 \times 2$  matrix  $T_b^a$ , with  $a, b = (0, 1)$ . A direct computation yields the two eigenvalues  $(T_a^a \pm \sqrt{W})/2$ , where  $W \equiv 2T_a^b T_b^a - (T_a^a)^2$ .

In the  $W > 0$  case  $T_b^a$  admits two real eigenvalues  $p_0 \neq p_1$ , associated with two orthonormal eigenvectors  $V_{(0,1)}^\alpha$  (with  $V_{(0)}^\alpha$  timelike). Hence altogether  $T_\beta^\alpha$  has four real eigenvalues  $p_\mu$  with orthonormal eigenvectors  $V_{(\mu)}^\alpha$ . In the Lorentz frame set by the tetrad  $V_{(\mu)}^\alpha$  the stress tensor is diagonal, with energy density  $\rho \equiv -p_0$  and three pressures  $p_i$ . This case is classified in Ref. [19] as type I. NEC is then satisfied iff  $\rho + p_i \geq 0$  for all  $i = 1, 2, 3$ , and WEC requires in addition  $\rho \geq 0$ .

In the  $W < 0$  case  $T_b^a$  has no real eigenvalues, marking a type IV [19] stress tensor. To analyze NEC we use double-null coordinates  $u, v$  ( $g_{uu} = g_{vv} = 0$ ), yielding  $W = 4(g^{uv})^2 T_{uu} T_{vv}$ . Introducing the two null vectors  $k^\alpha = (1, 0, 0, 0)$  and  $k^\alpha = (0, 1, 0, 0)$ , the two projections  $T_{\alpha\beta} k^\alpha k^\beta$  are just  $T_{uu}$  and  $T_{vv}$ . It follows that NEC is necessarily violated when  $W < 0$  — and so is WEC (a stronger condition).

Figure 2 displays  $W(r)$  (dashed curve) in Schwarzschild's Unruh state, showing that  $W > 0$  (i.e. type I) at  $r > r_0 \simeq 2.78M$ , and  $W < 0$  (type IV [41]) at  $2M < r < r_0$ . It also displays the various WEC/NEC indicators at  $r > r_0$  (recall that  $p_3 = p_2$  due to spherical symmetry). One finds that WEC and NEC break together, as the condition  $\rho + p_2 \geq 0$  is the first to be violated. This breakdown occurs surprisingly early, already at  $r = r_c \simeq 4.9M$ . It follows that both WEC

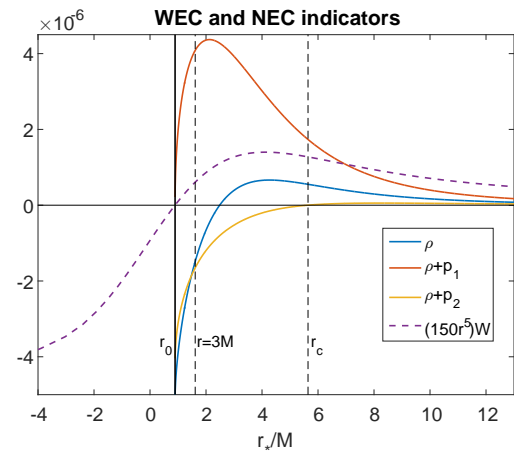


Figure 2: The various indicators for WEC and NEC, as a function of  $r_*$ . To the left of the solid vertical line  $r = r_0 \simeq 2.78M$  both WEC and NEC are violated as  $W < 0$ . To the right of  $r = r_0$ ,  $W$  is positive. NEC then demands  $\rho + p_1, \rho + p_2 \geq 0$ , and WEC also requires  $\rho \geq 0$ . It is clearly seen that  $\rho + p_2$  turns negative first (with decreasing  $r$ ), hence WEC and NEC break together. This happens at a surprisingly large radius  $r = r_c \simeq 4.9M$ . WEC and NEC are violated all the way from  $r_c$  to the horizon.

and NEC are violated throughout  $2M < r < r_c$ . [42]

*Observers along circular geodesics.*— It is interesting to compute the energy density measured by an observer moving along a circular geodesic. Assuming an equatorial geodesic, the projected energy density  $T_{ii} \equiv T_{\alpha\beta} u^\alpha u^\beta$  is

$$T_{ii}(r) = \frac{1}{1 - 3M/r} \left[ \frac{M}{r} T_\phi^\phi - \left( 1 - \frac{2M}{r} \right) T_t^t \right]. \quad (3)$$

Figure 3 plots this quantity as a function of  $r$ . It takes its maximum (positive) value at  $r \simeq 4.2M$  and becomes negative at  $r \lesssim 3.47M$ . These circular orbits with negative  $T_{ii}(r)$  are unstable as  $r < 6M$ . Nevertheless this is an interesting result, as one might hope that although WEC is violated an averaged version of it might still hold, but these circular geodesics obviously violate the averaged WEC (AWEC).

The family of timelike circular geodesics approach a null one as  $r \rightarrow 3M$ . At this limit  $T_{ii}(r)$  diverges, provided that the term in squared brackets in Eq. (3) is  $\neq 0$  at  $r = 3M$ . The dashed-dotted curve in Fig. 3 indicates that this quantity is indeed non-vanishing. In fact this limiting quantity is *negative*, suggesting that the  $r = 3M$  geodesic should violate ANEC. We shall now address this issue more directly.

*Violation of the ANEC.*— The most interesting circular orbit is the  $r = 3M$  null geodesic, as it is an elegant study case for the ANEC. Its tangent vector is  $k^\alpha = a(1, 0, 0, 1/\sqrt{27}M)$ , where  $a$  is an arbitrary con-

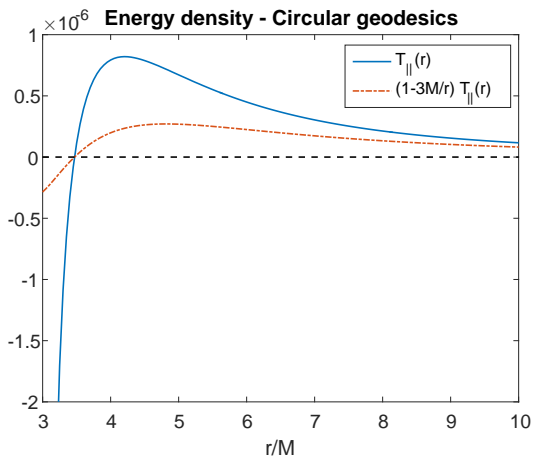


Figure 3: The projected energy density  $T_{||}(r)$  along a circular geodesic at radius  $r$ . It turns negative at  $r \lesssim 3.47M$ .

stant. The projected energy density is

$$T_{\alpha\beta}k^\alpha k^\beta = \frac{a^2}{3} \left[ T_\phi^\phi(r=3M) - T_t^t(r=3M) \right] \equiv T_{||}^{null}.$$

We calculated this quantity and found that

$$T_{||}^{null} \simeq -2.7 \cdot 10^{-7} a^2 \hbar M^{-4},$$

hence this geodesic violates NEC. Furthermore, since  $T_{\alpha\beta}k^\alpha k^\beta$  is constant along the circular orbit, the ANEC is violated too. This elegant counter-example implies that the ANEC is not a valid energy condition in semi-classical curved-spacetime scenarios, and in particular in BH evaporation.

*Discussion.*— We demonstrated the usage of our new mode-sum method for numerically computing the RSET in Schwarzschild background, for a MCMSF in the Unruh state. So far we developed three variants of this method:  $t$ -splitting for stationary backgrounds,  $\theta$ -splitting for spherically-symmetric backgrounds, and  $\varphi$ -splitting for axially-symmetric backgrounds. Since the Schwarzschild geometry enjoys all these symmetries, we have been able to compute the RSET in all three variants, and the results (Fig. 1) show nice mutual agreement.

These three variants complement each other in several ways. First, in some cases of interest two different variants may be used, which provides a strong consistency and accuracy check. One notable example is the Kerr case, in which both  $t$ - and  $\varphi$ -splittings are applicable. Another important example is the time-dependent spacetime of spherical evaporating BH. Actually this situation, of a spherical dynamical background, was our main motivation for developing this mode-sum approach. In this case both  $\theta$ - and  $\varphi$ -splittings should be applicable, which would allow cross-check of the results. Furthermore, in such a spherically-symmetric situation, the

$\varphi$ -splitting computation can be carried at various  $\theta$  values, each providing an independent consistency/accuracy test.

In addition, there are regions where one of the variants becomes inefficient or even inapplicable. This typically happens when the coordinate of symmetry which underlies the splitting direction becomes singular (or almost singular). For example, in the Schwarzschild case  $t$ -splitting deteriorates as one gets close to the horizon, and  $\varphi$ -splitting becomes inefficient at small  $\theta$  values. Having several different variants at our disposal allows more effective coverage of the various spacetime regions.

The  $\varphi$ -splitting variant, which was presented here for the first time, is a powerful method in its own right. The details of this variant will be presented elsewhere. It should eventually allow investigation of the dynamical evaporation process of *spinning BHs* as well. To this end, however, we shall first have to resolve the difficulties that this variant presently faces at small  $\theta$  values.

The other objective of this paper was the status of various energy conditions in the spacetime outside a spherical evaporating BH. The local violation of WEC and NEC by quantum fields is well known; and indeed we found that both WEC and NEC are violated throughout  $2M < r < r_c \simeq 4.9M$ . Here we showed, however, that *ANEC is violated too* (and the same for AWEC). In particular, the orbit  $r = 3M$  violates ANEC. Such violations were already demonstrated [22, 23] for conformally coupled fields, and here we showed it for the first time (to our knowledge) for a MCMSF.

In fact, this ANEC violation is not limited to the strict  $r = 3M$  circular geodesic: Consider a “Zoom-whirl” null geodesic which arrives from infinity and makes a sufficiently large number of revolutions  $N$  around the BH near  $r = 3M$ , before escaping back to infinity. The ANEC integrand in (2) should be positive at sufficiently large  $r$ , but it takes an approximately-constant negative value ( $\approx T_{||}^{null}$ ) near  $r = 3M$ . As  $N$  exceeds some critical value  $N_c$  (independent of  $M$ ), the negative contribution will surely dominate, because it is  $\propto N$ . Such unbound null geodesics will violate the ANEC too.

Strictly speaking, this ANEC violation was only shown here for pure Schwarzschild background. However, such violation must also occur in *evaporating BHs*. The local backreaction effects on the metric of an evaporating BH should be  $\propto \langle T_{\alpha\beta} \rangle_{ren} \propto \hbar/M^4$ . Consider now a Zoom-whirl null geodesic which makes, say,  $N = 2N_c$  revolutions at  $r \cong 3M$  around an evaporating BH of (current) mass  $M$ . We denote by  $\Delta t$  the  $t$ -interval required for making these  $2N_c$  revolutions ( $\Delta t \approx 12\pi\sqrt{3}N_cM$ ). We can now choose a sufficiently large  $M$ , such that the BH evaporation time ( $\propto M^3$ ) is  $\gg \Delta t \propto M$ . The aforementioned Zoom-whirl geodesic will hardly be affected by the local backreaction on the metric, and the same for the ANEC integrand, hence ANEC violation should occur in this case too.

Note that such ANEC violation should also occur if the BH is spinning, at least if the spin is not too large, just by continuity. It remains to investigate whether ANEC violation also occurs in rapidly-spinning evaporating BHs. Another interesting research direction is using the RSET results to examine Quantum Inequalities [30–34].

It should be noted that a weaker averaged energy condition exists, the so-called *achronal averaged null energy condition*. This condition is sufficient [26] to prevent certain exotic phenomena. Kontou and Olum [35] further argued that this energy condition is guaranteed to hold (for MCMSF) in self-consistent semiclassical curved spacetimes. The Schwarzschild’s  $r = 3M$  geodesic does not provide a counter example of course, as it is not achronal.

*Acknowledgment.*— We would like to thank Thomas Roman and Matt Visser for drawing our attention to Refs. [22] and [23] respectively. We are also grateful to Paul Anderson for numerous interesting and useful discussions. This research was supported by the Asher Fund for Space Research at the Technion.

- 
- [1] S. W. Hawking, *Commun. Math. Phys.* **43**, 199 (1975).  
 [2] B. S. DeWitt, *Dynamical Theory of Groups and Fields* (Gordon and Breach, New York, 1965).  
 [3] S. M. Christensen, *Phys. Rev. D* **14**, 2490 (1976).  
 [4] P. Candelas and K. W. Howard, *Phys. Rev. D* **29**, 1618 (1984).  
 [5] K. W. Howard, *Phys. Rev. D* **30**, 2532 (1984).  
 [6] P. R. Anderson, *Phys. Rev. D* **41**, 1152 (1990).  
 [7] P. R. Anderson, W. A. Hiscock, and D. A. Samuel, *Phys. Rev. D* **51**, 4337 (1995).  
 [8] See also G. Duffy and A. C. Ottewill, *Phys. Rev. D* **77**, 024007 (2008) for a related work in Kerr.  
 [9] C. Breen and A. C. Ottewill, *Phys. Rev. D* **85**, 084029 (2012).  
 [10] C. Breen, M. Hewitt, E. Winstanley and A. C. Ottewill, *Phys. Rev. D* **92**, 084039 (2015).  
 [11] A. C. Ottewill and P. Taylor, *Phys. Rev. D* **82**, 104013 (2010).  
 [12] A. C. Ottewill and P. Taylor, *Class. Quant. Grav.* **28**, 015007 (2011).  
 [13] A. Levi and A. Ori, *Phys. Rev. D* **91**, 104028 (2015).  
 [14] A. Levi and A. Ori, *Phys. Rev. D* **94**, 044054 (2016).  
 [15] A. Levi and A. Ori (In preparation).  
 [16] T. Elster, *Phys. Lett.* **94** A, 205 (1983).  
 [17] B. P. Jensen, J. G. McLaughlin, and A. C. Ottewill, *Phys. Rev. D* **43**, 4142 (1991).  
 [18] M. Visser, *Class. Quant. Grav.* **17**, 3843 (2000).  
 [19] S. W. Hawking and G. F. R. Ellis, *The Large Scale Structure of Space-Time* (Cambridge University Press, 1973).  
 [20] G. Klinkhammer, *Phys. Rev. D* **43**, 2542 (1991).  
 [21] J. L. Friedman, K. Schleich, and D. M. Witt, *Phys. Rev. Lett.* **71**, 1486 (1993).  
 [22] L. H. Ford and T. A. Roman, *Phys. Rev. D* **53** 1988, (1996).  
 [23] M. Visser, *Phys. Rev. D* **56**, 936 (1997).  
 [24] See also M. Visser, *Phys. Rev. D* **54**, 5103 (1996), and M. Visser, *Phys. Rev. D* **54**, 5116 (1996), for Hartle-Hawking and Boulware states respectively.  
 [25] C. J. Fewster, K. D. Olum, and M. J. Pfenning, *Phys. Rev. D* **75**, 025007 (2007).  
 [26] N. Graham and K. D. Olum, *Phys. Rev. D* **76**, 064001 (2007).  
 [27] W. G. Unruh, *Phys. Rev. D* **14**, 870 (1976).  
 [28] P. Martín-Moruno and M. Visser, *High Energ. Phys.* **1309**, 050 (2013).  
 [29] P. Martín-Moruno and M. Visser, arXiv:1510.00158.  
 [30] L. H. Ford, *Phys. Rev. D* **43**, 3972, (1991).  
 [31] L. H. Ford and T. A. Roman, *Phys. Rev. D* **48**, 776 (1993).  
 [32] L. H. Ford and T. A. Roman, *Phys. Rev. D* **51**, 4277 (1995).  
 [33] C. J. Fewster and C. J. Smith, *Ann. Henri Poincaré* **9**, 425 (2008).  
 [34] E. A. Kontou and K. D. Olum, *Phys. Rev. D* **91**, 104005 (2015).  
 [35] E. A. Kontou and K. D. Olum, *Phys. Rev. D* **92**, 124009 (2015).  
 [36] Throughout this paper units  $c = G = 1$  are used, along with signature  $(-+++)$ .  
 [37] For more recent works on regularization (still in the Euclidean sector) see [9–12].  
 [38] Here  $t, r, \theta, \varphi$  are standard flat-spacetime spherical coordinates at asymptotically-flat infinity.  
 [39] Non-minimally coupled scalar fields may violate all standard energy conditions (including ANEC) even classically [18].  
 [40] In all figures, numerical values are expressed in units of  $\hbar/M^4$ .  
 [41] For earlier observations of type-IV RSET see [28, 29].  
 [42] At the transition point  $r = r_0$  WEC/NEC are violated too, and the RSET there is type II.